South-coast cyclone in Japan during El Niño-caused warm winters

Hiroaki Ueda[1,*], Yuusuke Amagai[1] and Masamitsu Hayasaki[2]

[1]University of Tsukuba, 1-1-1 Tennodai, Tsukuba, Ibaraki 305-8572, Japan

[2]National Institute for Environmental Studies, 16-2 Onogawa, Tsukuba, Ibaraki 305-8506, Japan

Submitted to *Asia-Pacific Journal of Atmospheric Sciences*

September 20, 2016

Revised December 22, 2016

*Dr. Hiroaki UEDA
Faculty of Life and Environmental Sciences
University of Tsukuba, Tsukuba, Ibaraki 305-8572, Japan
Phone:+81 (29) 853-4756; Fax: +81(29) 853-6879
E-mail: ueda.hiroaki.gm@u.tsukuba.ac.jp

Abstract:

La Niña conditions during boreal winter sometimes brings excessive snowfall in Japan, especially on the East Sea/Sea of Japan coastal and mountain areas through intensified northwesterly cold winds caused by La-Niña related atmospheric teleconnection. Meanwhile, snowfall events also increase in the Pacific coast area of Japan during the El Niño state due to extratropical cyclones passing along the south coast of Japan (hereafter referred to as South-coast cyclone). In the present study, we investigated year-to-year snowfall/rainfall variations based on meteorological station data and cyclone tracks identified by using the Japanese 55-year Reanalysis. The result clearly indicates increase of the South-coast cyclone during El Niño-developing winters, which is consistent with excessive snowfall in the northern part of the Pacific coast. Strong subtropical jet hampers cyclogenesis due to less vertical interaction through the trapping of upper-level eddies. During El Niño-developing winters, the subtropical jet is weakened over East Asia, indicating dynamic linkage to increased cyclone frequency. In addition to this, both the deepening of the upper-tropospheric trough over East Asia and anomalous low-tropospheric northwest anticyclones extending from the Philippines

toward Japan are also consistent with the enhancement of cyclogenesis over the East China Sea as well as warm winter in Japan.

Key words: South-coast cyclone, excessive snowfall, ENSO, teleconnection

1. Introduction

Japan is known as one of the southern limits of heavy snowfall in the world. Climatologically, snowfall along the East Sea/Sea of Japan, including the mountainous regions, is closely associated with the East Asian winter monsoon (EAWM), which originates from the Siberian high and converges into the Aleutian low (Matsumoto, 1992). The relatively drier and colder air mass becomes more unstable stratification through the absorption of a large amount of moisture evaporated from the East Sea/Sea of Japan (Manabe, 1957), which brings heavy snowfall over the backbone range of the Japanese Islands. Therefore, variations of snowfall associated with cyclone activities are of great scientific and social importance, attracting much attention in view of the cold air outbreaks related to the EAWM toward the subtropics as well as the tropics (e.g., Chang et al., 1980; Zhang et al., 1997; Gong et al. 2014).

The modulation of the EAWM depends upon several factors. Among these, the Arctic Oscillation (AO) is a major candidate. Wang et al. (2010) showed that the Northern mode of EAWM has close relationship with AO, particularly after 1970s

(Yun et al. 2014). Whilst several studies have shown that the AO and the main body of EAWM are almost independent of each other (Wu and Wang, 2002; Kawamura and Ogasawara, 2007; Nan and Zhao, 2012), requiring alternative physical processes. Recently, Ueda et al. (2015) revealed that anomalous convection in the tropical western Pacific during La Niña events (a cold episode of El Niño) can explain the enhancement of a northwesterly wind embedded in the EAWM together with intensified low pressure over and around Japan through an atmospheric teleconnection of tropical origin. The reverse is almost true in the case of El Niño, which favors less snowfall on the East Sea/Sea of Japan coast.

In contrast to the East Sea/Sea of Japan coast, the Pacific coast is characterized by fine weather through the mountain-caused Föhn phenomenon. Meanwhile, South-coast cyclone originating from the East China Sea, which travel eastward over the Kuroshio region along the south coast of Japan, occasionally bring wet snowfall over the Pacific coast region, including cosmopolitan areas, such as Tokyo. From the social point of view, an occasional excessive snowfall over the Pacific coastal area could potentially affect socio-economic activity by, among other things, obstructing traffic and damaging agriculture. It has been widely known that the winter air temperature in Japan becomes relatively warmer during warm El Niño episodes, which are characterized by weakened EAWMs (e.g., Wang et al., 2000). The anomalous climate state around Japan is consistent with a reduction of the east-west pressure gradient around Japan. Consequently, anomalous low-pressure field emerges over the Northwest Pacific to the south of Japan, which may give rise to generation of the South-coast cyclone through northward advection of warm and moist air. It has been revealed that the Pacific storm track during the El Niño shifts equatorward in response to the changed in the subtropical jet relevant to modulation of the Hadley circulation (e.g., Trenberth and Hurrell, 1997; Straus and Shukla, 1997). These changes cause downward development of storm track and resultant enhancement of cyclogenesis (Chang et al, 2002). Numerous studies have greatly advanced our knowledge of the influence of ENSO or AO on EAWM (e.g., Wang et al. 2010, Yun et al. 2014) including precipitation change (Ropelewski and Halpert, 1987). The other teleconnection pattern such as North Atlantic Oscillation (Ueno, 1992) or Eurasian pattern (Tachibana et al., 2007) also affects the South-coast cyclone. Yamazaki et al (2015) revealed the influence of atmospheric blocking over the northwestern Pacific on heavy snowfall events in Japan through intrusion of cold air mass from the polar region and resultant changes in cyclogenesis. Observed changes in the cyclones especially obtained from cyclone-tracking method (see methods), however, cannot establish statistical and physical explanation between the South-coast cyclone and amount of rainfall/snowfall in Japan. Therefore, the aim of the present study is to identify cyclone activities, especially focusing on the South-coast cyclone along the south coast of Japan from the perspective of ENSO fluctuations.

2. Data and Methods

Procedures for identifying and tracking cyclones were based on Serreze et al. (1993) and have been used in some previous studies (Hayasaki and Kawamura, 2012; Hayasaki et al., 2013). As noted in these studies, the cyclone-tracking algorithm is good enough to detect individual cyclones and to trace their paths with the exception of small-scale cyclones (e.g., secondary cyclones along a front, thermal lows in land areas). Because the details of cyclone tracking procedures have been mentioned in previous studies, we overview them only briefly. Sea level pressure data on linear lat-lon grids were converted into the Equal-Area Scalable Earth (EASE) grid, which has 145x145 grids with a 125-km interval at the North Pole (Fig. 1). The cyclone center was identified by the SLP minimum, which is smaller than or equal to 0.5 hPa in the surrounding grids. Cyclone centers identified in successive time steps were connected if the cyclone center candidate was located within four grids of the target centers in the previous time step. Long-term SLP data taken every six hours was obtained from the Japanese 55-year Reanalysis (JRA-55) from 1958–2016 (Kobayashi et al., 2015).

Now, we focus on the South-coast cyclone along the south coast of Japan. It is well known that the South-coast cyclone typically originates in the East China Sea and move eastward-northeastward along the Kuroshio (cf., Nakamura et al., 2012). The cyclone tracks were selected by the geographical paths of identified cyclones that travel in the southern part of the Japanese Islands (the surrounding area in Fig.

1). We also used the daily rainfall and snowfall in Japan (149 stations) provided by the Japan Meteorological Agency for the period between 1961 and 2016.

3. South-coast cyclone and the ENSO

a. Observed rainfall/snowfall anomalies

The year-to-year variation of the multivariate ENSO index (MEI) based on six observed variables over the tropical Pacific (Wolter and Timlin, 2011) is shown in Fig. 2. The positive (negative) values indicate the El Niño (La Niña) state. During the last 56 years (1961–2016), we choose the top 10 El Niño (open circles) and La Niña (open triangle) events. Based on these criteria, we examined the composite differences in the cyclone track frequencies between El Niño and La Niña conditions. Climatologically, South-coat cyclone is generated in the East China Sea and moves northeastward along the Kuroshio, having its peak to the south of Kanto-plain including Tokyo. During El Niño years (Fig. 3b), cyclone track frequencies are relatively large over the Pacific, especially off of Japan’s south coast as compared with those in La Niña years (Fig. 3c). The salient anomalies are recognizable in the composite differences between El Niño and La Niña (Fig. 3d). The same analysis was applied for rainfall (Fig. 4a) and snowfall (Fig. 4b). A distinct contrast can be seen between the Pacific coastal area and the East Sea/Sea of Japan coast with the exception of Hokkaido (Japan's northern big island). Rainfall anomalies are positive along the Pacific coast, while they are negative along the East Sea/Sea of Japan coast; this is consistent with the cyclone track frequencies. Rainfall and snowfall anomalies in Tokyo during El Niño show a 30% increase relative to La Niña (Table 1). A significance test for employing Student's statistics confirmed that those increasing and decreasing tendencies in regional rainfall and snowfall are significant at the 5% level. A slight month-to-month difference is recognizable in winter, while the DJF-mean better characterizes the relationship between cyclone track frequencies and rainfall/ snowfall variations throughout the winter season. This is due to the prolonged anomalous anticyclone over the tropical Northwest Pacific caused by the mature stage of El Niño together with Kelvin-wave divergence anchored with delayed basin-wide warming of Indian Ocean in the El Niño winter (Xie et al., 2016).

Taking a closer look at the regional differences in snowfall anomalies, one may notice that the values are relatively small in the southern part of Japan facing the Pacific Ocean. This can be attributed to the relatively warmer air temperatures as compared with those in the northern part of Japan. In other words, distinct snowfall anomalies are recognizable in the area north of Tokyo, including the northeastern provinces, called the *Kanto* area.

b. Physical background for the modulation of cyclone track frequencies

The present study concerns how cyclone track frequencies are modulated in relation to the ENSO condition. Figure 5 shows the composite anomalies of the circulation fields of the major (top 10) El Niño minus La Niña events. In the upper troposphere (Fig. 5a), twin anomalous anticyclones are recognizable over the tropical eastern Pacific, striding across the equator, accompanied by warmer air temperatures. This is a typical atmospheric Rossby response caused by the enhanced convection relevant to the underlying warm SST anomalies (Matsuno, 1966; Gill, 1980). As for East Asia, the mid-latitude trough embedded in the westerly jet intrudes the subtropics to the southwest of Japan, which is consistent with the increased track frequencies in Fig. 3d. Another noticeable feature in Fig. 5a is the presence of zonally elongated cold temperature anomalies over East Asia along a latitudinal band of 30°–45°N, which corresponds with the upper-level trough centered around 120°–140°E.

In the lower-troposphere (Fig. 5b), the anomalous Pacific anticyclone dominates to the east of Philippines, stretching in the northeast direction toward the southeast of Japan. The northeasterly wind anomalies emerging to the southwest of Japan indicate the weakening of the East Asian winter monsoon. Positive temperature anomalies extending from the South China Sea to Japan in Fig. 5b are consistent with the attenuated EAWM. As shown in Fig. 6a and Table 1, northeastward transport of moisture toward Japan during the El Niño shows significant increase along the western periphery of anomalous anticyclone dominating over the Northwest Pacific (see Fig, 5b). These features are consistent with increase of the South-coat cyclone (see Fig. 3d) and resultant warm advection extending to the Northwest Pacific around the dateline (Fig. 6b). Wang et al. (2000) have proposed that lower-tropospheric northwest Pacific anticyclones tend to persist during El Niño years due to underlying cold SST anomalies through local air-sea interaction. In addition to this, basin-wide warming in the Indian Ocean after the peak phase of El Niño also contributes to maintaining the northwest Pacific anticyclone by means of the propagation of tropospheric Kelvin waves (Xie et al., 2016). Thus, warm winters in Japan and enhanced cyclones to the south of Japan can be dynamically interpreted by ENSO-caused anomalous global circulation.

c. The subtropical jet and storm track

Previous subsections have focused on the influence of tropical-origin teleconnections on cyclone activities to the south of Japan (30°–35°N). Climatologically, strong westerlies, which are called the subtropical jet (hereafter abbreviated as STJ), dominate in that region (Fig. 7). Baroclinic eddies are generated in the vertically sheared STJ, which is also an important factor for the modulation of storm tracks, including the South-coast cyclone, to the south of Japan. It has been revealed dynamically that cyclones rapidly develop through eddy coupling between the upper troposphere and the lower troposphere (Takayabu, 1991). Climatologically, Nakamura and Sampe (2002) found that the strong STJ weakens eddy amplification through the trapping of upper-level eddies. This relationship is manifested as “midwinter suppression” (Nakamura, 1992). It is conceivable that the reverse could be applicable to the attenuated STJ condition. Figure 7 shows the composite anomalies of the zonal wind (shading) between major El Niño and La Niña events. If we pay attention to the core region of the STJ around 30°–35°N (see also Table 1), corresponding to the cyclone south of Japan, we notice the weakened STJ (blue shading) in the upper troposphere. This is consistent with the cold anomalies seen in Fig. 5a, due to less zonal warm advection in the STJ. Furthermore, it could also be responsible for the increase in cyclones to the south of Japan by means of intensified vertical eddy coupling. In addition to the eddy-mean flow interaction, Lee et al. (2011) revealed that increase in moisture in upstream region of storm tracks has also crucial role in the enhancing of storm track activities. As was shown in Table1, the additional moisture into the storm track regions during the El Niño is consistent with increase of the South-coast cyclone.

4. Discussion and Remarks

We examined long-term (1961–2016) rainfall/snowfall variations in view of ENSO-caused circulation changes and the resultant cyclogenesis along the Pacific coast of Japan. During El Niño years, the northwest Pacific anticyclone develops in the lower troposphere to the east of the Philippines, which manifests as a warm winter caused by the weakened EAWM. In contrast, an upper-tropospheric trough is generated over the continental area of East China through the East China Sea, which could facilitate enhanced cyclogenesis and more rainfall/snowfall ensuing along the Pacific coast (Table 1). These results are consistent with excessive snowfall along the East Sea/Sea of Japan coast, including the backbone mountain regions in Japan, associated with intensified EAWM during La Niña years (Ueda et al., 2015). Thus, the contrast in the amounts of snowfall of El Niño and La Niña as well as the opposite relationship between the East Sea/Sea of Japan coast and the Pacific coast could be explained by the intensity of the EAWM and the South-coast cyclone.

Regarding snow accumulation events in Tokyo, Tachibana et al. (2007) revealed a crucial role of the Eurasian pattern, which is the response to low-pressure anomalies dominant over the entire region of Japan, including East China. Their obtained cyclonic anomaly was located slightly to the north (~40°N) of the present study (~30°N). Because their study starts from the year-to-year snow accumulation in Tokyo, it is conceivable that their result includes the anomalous cyclonic circulation over and around Japan that emerges in both El Niño and La Niña. In addition to this, we should mention the behavior of the subtropical jet (STJ; 30°~35°N). Nakamura and Sampe (2002) showed that a stronger STJ hampers the development of cyclones by trapping upper-level eddies. In fact, the composite anomalies of zonal winds during El Niño (Fig. 7) show a weaker STJ, which is consistent with the increase in cyclones to the south of Japan. Developing a predictive understanding of regional snowfall/rainfall variations is fundamentally important missions, which is expected to connect the global climate research community and meso-scale researchers. From this perspective combination of meso-scale model and global circulation model, which resolves synoptic disturbances, could lead to improve the seasonal forecast skill.

The ENSO has decadal variability such as the Pacific inter-decadal oscillation (PDO; Mantua et al. 1997). In the present study we examined the differences in cyclone track between the positive and negative phase of PDO, while we do not obtain the significant relationship (not shown). As for the long-term change, the total number of extratropical cyclone is projected to decrease in a warmed climate due to reduction of baroclinicity near the surface (Mizuta et al., 2011). Whilst the most climate models show El Niño-like warming pattern (e.g., Endo et al. 2012), which potentially affects the number of South-coast cyclone. Further study is needed to clarify the influence of global warming on cyclogenesis and its passage from rainfall/snowfall variation perspective.

Acknowledgements

The authors are grateful for the editors and anonymous reviewers giving us the opportunity to submit this manuscript. This work was supported by the Environment Research and Technology Development Fund (A-1201) of the Ministry of the Environment, Japan, and by the Program for Risk Information on Climate Change (SOUSEI program) from the Ministry of Education, Culture, Sports, Science and Technology (MEXT) of Japan.

References

Chang, C.-P., and K. M. W. Lau, 1980: Northeasterly cold surges and near-equatorial disturbances over the Winter MONEX area during December 1974. Part II: Planetary-scale aspects. *Mon. Wea. Rev.*, **108**, 298–312.

Chang, E. K. M., S. Lee and K. L. Swanson, 2002: Storm track dynamics, *J. Climate*, **15**, 2163-2183.

Endo, H., A. Kitoh, T. Ose, R. Mizuta, and S. Kusunoki, 2012: Future changes and uncertainties in Asian precipitation simulated by multi-physics and multi-sea surface temperature ensemble experiments with high-resolution Meteorological Research Institute atmospheric general circulation models (MRI-AGCMs). *J. Geophys. Res.*, **117**, D16118.

Gill, A. E., 1980: Some simple solutions for heat-induced tropical circulation. *Quart. J. Roy. Meteor. Soc.*, **106**, 447-462.

Gong, H., L. Wang, W. Chen, R. Wu, K. Wei, and X. Cui, 2014: The climatology and interannual variability of the East Asian winter monsoon in CMIP5 models, *J. Climate*, **27**, 1659–1678, doi:10.1175/JCLI-D-13-00039.1.

Hayasaki, M., and R. Kawamura, 2012: Cyclone activities in heavy rainfall episodes in Japan during spring season. *SOLA*, **8**, 45–48, DOI: 10.2151/sola.2012-012.

Hayasaki, M., R. Kawamura, M. Mori, and M. Watanabe, 2013: Response of extratropical cyclone activity to the Kuroshio meander in northern winter. *Geophys. Res. Lett.*, **40**, DOI: 10.1002/grl.50546.

Kawamura, R., and T. Ogasawara, 2007: Characteristics of large-scale atmospheric circulations associated with the heavy winter snowfall of 2005/06. *J. Jpn. Soc. Snow Ice (Seppyo)*, **69**, 21–29 (in Japanese with English abstract).

Kobayashi, S., Y. Ota, Y. Harada, A. Ebita, M. Moriya, H. Onoda, K. Onogi, H. Kamahori, C. Kobayashi, H. Endo, K. Miyaoka, and K. Takahashi, 2015: The JRA-55 Reanalysis: General specifications and basic characteristics. *J. Meteor. Soc. Japan*, **93**, 5–48.

Lee, S.-S. et al., 2011: A comparison of climatological subseasonal variations in the wintertime storm track activity between the North Pacific and Atlantic: local energetics and moisture effect. *Clim Dyn.*, **37**, 2455-2469.

Matsuno, T., 1966: Quasi-geostrophic motions in the equatorial area. *J. Meteor. Soc. Japan*, **44**, 25-43.

Manabe, S., 1957: On the Modification of Air-mass over the Japan Sea when the Outburst of Cold Air Predominates. *J. Meteor. Soc. Japan*, **35**, 311–326.

Mantua, N. J., S. R. Hare, Y. Zhang, J. M. Wallace, and R. C. Francis, 1997: A Pacific interdecadal climate oscillation with impacts on salmon production, *Bull. Amer. Meteor. Soc*., **78**, 1069–1079, doi:10.1175/1520-0477(1997)078.

Matsumoto, J., 1992: The seasonal changes in Asian and Australian monsoon regions. *J. Meteor. Soc. Japan*, **70**, 257–273.

Mizuta, R., M. Matsueda, H. Endo, and S. Yukimoto, 2011: Future change in extratropical cyclones associated with change in the upper troposphere. *J. Climate*, **24**, 6456-6470.

Nakamura, H., 1992: Midwinter suppression of baloclinic wave activity in the Pacific. *J. Atmos. Sci.*, **49**, 1629–1642.

Nakamura, H., and T. Sampe, 2002: Trapping of synoptic-scale disturbances into the North-Pacific subtropical jet core in midwinter. *Geophys. Res. Lett.*, **29**, DOI: 10.1029/2002GL015535.

Nakamura, H., A. Nishina, and S. Minobe, 2012: Response of storm tracks to bimodal Kuroshio path states south of Japan. *J. Climate*, **25**, 7772–7779.

Nan, S., and P. Zhao, 2012: Snowfall over central-eastern China and Asian atmospheric cold source in January. *Int. J. Climatology*, **32**, 888–899.

Ropelewski, C. F., and M. S. Halpert, 1987: Global and regional scale precipitation patterns associated with the El Niño/Southern Oscillation. *Mon. Wea. Rev.*, **115**, 1606–1626.

Serreze, M. C., J. E. Box, R. G. Barry, and J. E. Walsh, 1993: Characteristics of Arctic synoptic activity, 1952-1989. *Meteorol. Atmos. Phys.*, **51**, 147–164.

Straus, D. M. and J. Shukla 1997, Variations of midlatitude transient dynamics associated with ENSO, *J. Atmos. Sci.*, **54**, 777-790.

Tachibana, Y., T. Nakamura, and N. Tazou, 2007: Interannual variation in snow-accumulation events in Tokyo and its relationship to the Eurasian pattern. *SOLA*, **3**, 129–132, DOI:10.2151/sola.2007-033.

Takayabu, I., 1991: “Coupling Development”: An efficient mechanism for the development of extratropical cyclones. *J. Meteor. Soc. Japan*, **69**, 609–628.

Trenberth, K. E. and W. Hurrell, 1994: Decadal atmosphere-ocean variations in the Pacific. *Clim. Dyn*., **9**, 303-319.

Ueda, H., A. Kibe, M. Saitoh, and T. Inoue, 2015: Snowfall variations in Japan and its linkage with tropical forcing. *Int. J. Climatol.*, **35**, 991-998.

Ueno, K., 1993: Inter-annual variability of surface cyclone tracks, atmospheric circulation patterns, and precipitation patterns, in winter. *J. Meteor. Soc. Japan*, **71**, 655-671.

Wang, B., R. Wu, and X. Fu, 2000: Pacific-East Asian teleconnection: How does ENSO affect East Asian climate? *J. Climate*, **13**, 1517–1536.

Wang, B. et al., 2010: Another look at interannual-to-interdecadal variations of the East Asian winter monsoon: the Northern and Southern temperature modes. *J. Climate*, **23**, 1495-1512.

Wolter, K. and M. S. Timlin, 2011: El Niño/Southern Oscillation behaviour since 1871 as diagnosed in an extended multivariate ENSO index (MEI.ext), *Int. J. Climatol.*, **31**, 1074-1087, DOI: 10.1002/joc.2336.

Wu, B., and J. Wang, 2002: Winter Arctic Oscillation, Siberian High, the East Asian winter monsoon. *Geophys. Res. Lett.*, **29**, 1897, DOI: 10.1029/2002GL015373.

Xie, S.-P., Y. Kosaka, Y. Du, K HU, J. S. Chowdary, and G. Huang, 2016: Indo-Western Pacific Ocean capacitor and coherent climate anomalies in post-ENSO summer: A Review. *Adv. Atmos. Sci*, 33, 411–432.

Yamazaki, A., M. Honda and A. Kuwano-Yoshida, 2015: Heavy snowfall in Kanto and on the Pacific Ocean side of northern Japan associated with western Pacific blocking. *SOLA*, **11**, 59-64.

Yun, K.-S. et al., 2014: Interdecadal changes in the Asian winter monsoon variability and its relationship with ENSO and AO. Asia-Pacific *J. Atmos. Sci*., **50**, 531-540.

Zhang, Y., K. R. Sperber, and J. S. Boyle, 1997: Climatology and interdecadal variation of the East Asian winter monsoon: results from the 1979-95 NCEP/NCAR Reanalysis, *Mon. Wea. Rev*., **125**, 2605–2619.

Tables

Table 1. DJF composited anomalies between the top 10 El Niño minus La Niña events. Bold indicates a confidence level > 95%. Rainfall and snowfall anomalies were provided by the Tokyo Meteorological Observatory. Horizontal advection (*v'T'*) at 850 hPa and vertically (1000-1hPa) integrated moisture flux is the area average over 25°–35°N and 120°–140°E. The STJ is a zonal wind component at 200 hPa averaged over 30°–35°N and 120°–140°E.

Figures

Fig. 1. Division of an area of cyclone tracks. Red (south of Japan) demarcates the subject area in the present study for examining the relationship between rainfall/snowfall variations in the Pacific coast of Japan and cyclone tracks along the south coast of Japan.

Fig. 2. Time series of the interannual variation of the multivariate ENSO index (MEI) between 1961 and 2016. Open circles and triangles show the top 10 El Niño and La Niña events, respectively.

Fig. 3. DJF cyclone track frequencies (count month^{-1}). (a) Climatological mean (1981–2010). (b) and (c) are composite anomalies of major El Niño events and La Niña events, respectively. (d) The difference between major El Niño minus La Niña events. Grids with a confidence level of > 95% are denoted by dot. The total number of South-coast cyclone between December and February is denoted in the upper-right.

Fig. 4. Composited anomalies between the major El Niño and La Niña for total amounts of (a) rainfall and (b) snowfall in boreal winter. The values are three-month integration of daily-based data. Stations with a confidence level of > 95% are denoted by dot.

Fig. 5. Same as Fig. 4 but for stream function (contours: positive indicates anti-cyclone in the Northern Hemisphere) and temperature (shading); (a) 200 hPa, (b) 1000 hPa. Areas with a confidence level of > 95% are denoted by oblique line.

Fig. 6. Same as Fig. 4 but for (a) vertically integrated moisture flux (*q'u', q'v'*) in the lower troposphere (1000-1hPa) and (b) horizontal heat advection (*v'T'*) at 850 hPa. Areas with a confidence level of > 95% are denoted by oblique line.

Fig. 7. Latitude-height section of the zonal mean u-wind (m s^{-1}) across Japan, showing the STJ. Shading denotes composited anomalies between the major El Niño and La Niña. Contours indicate the climatology. Areas with a confidence level of > 95% are denoted by oblique line.

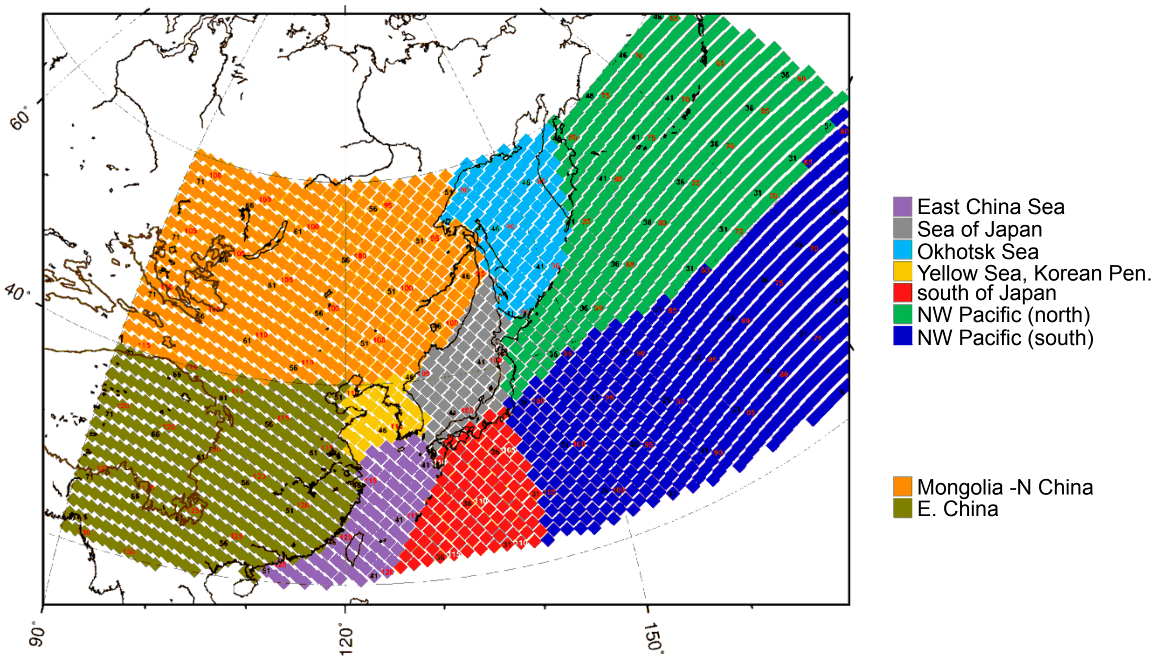

Fig. 1. Division of an area of cyclone tracks. Red (south of Japan) demarcates the subject area in the present study for examining the relationship between rainfall/snowfall variations in the Pacific coast of Japan and cyclone tracks along the south coast of Japan.

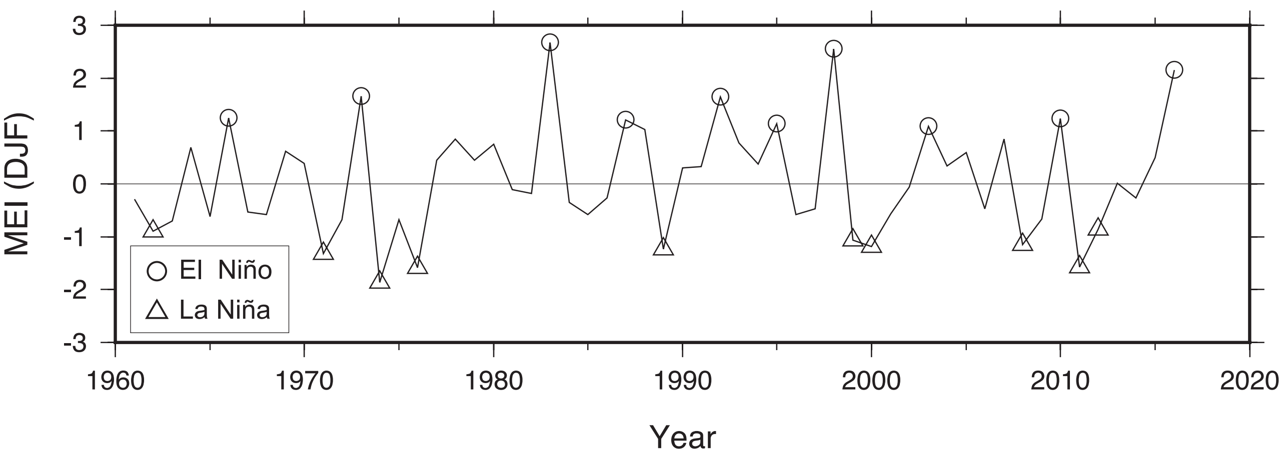

Fig. 2. Time series of the interannual variation of the multivariate ENSO index (MEI) between 1961 and 2016. Open circles and triangles show the top 10 El Niño and La Niña events, respectively**.**

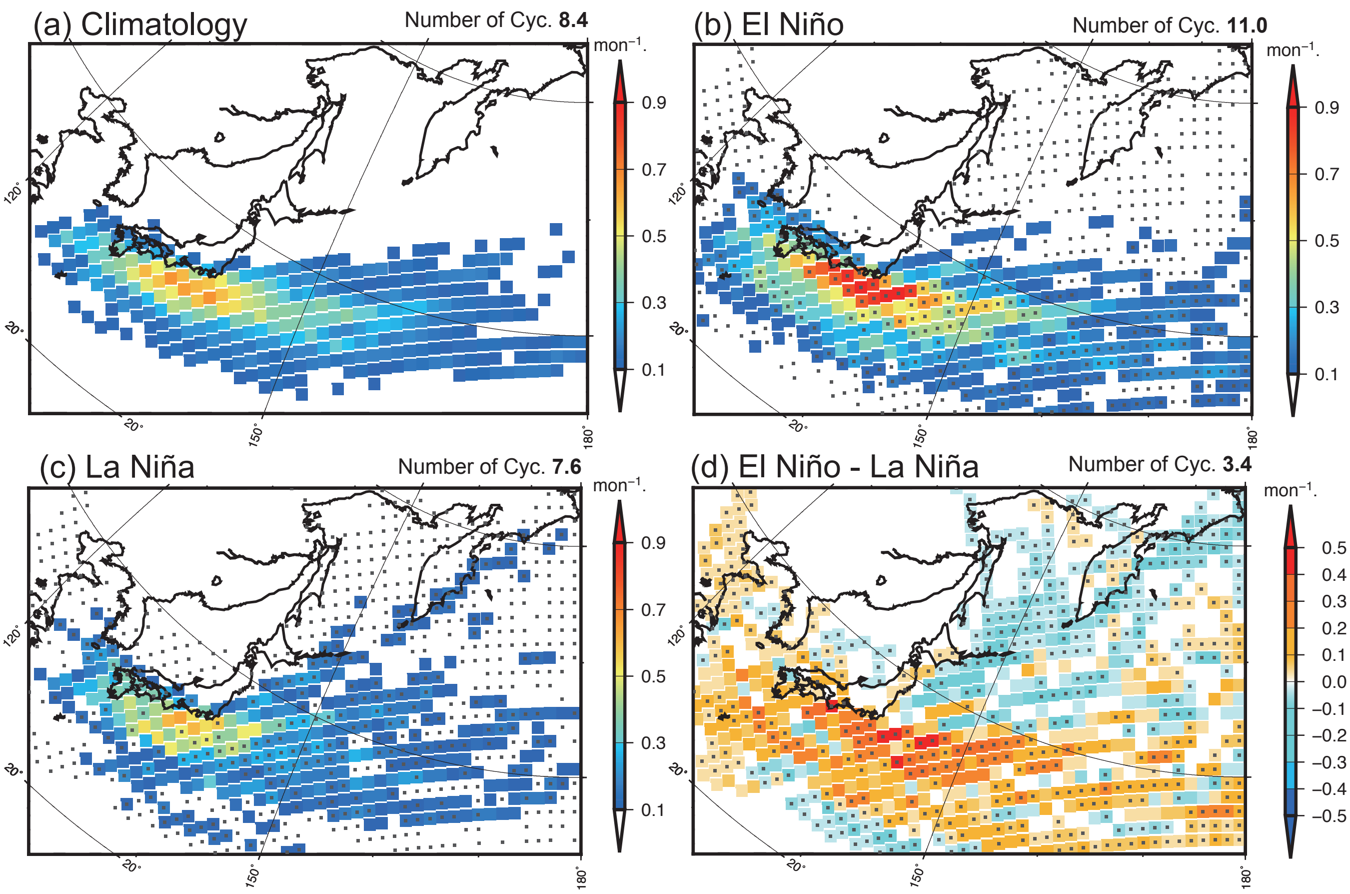

Fig. 3. DJF cyclone track frequencies (count month-1). (a) Climatological mean (1981–2010). (b) and (c) are composite anomalies of major El Niño events and La Niña events, respectively. (d) The difference between major El Niño minus La Niña events. Grids with a confidence level of > 95% are denoted by dot. The total number of South-coast cyclone between December and February is denoted in the upper-right.

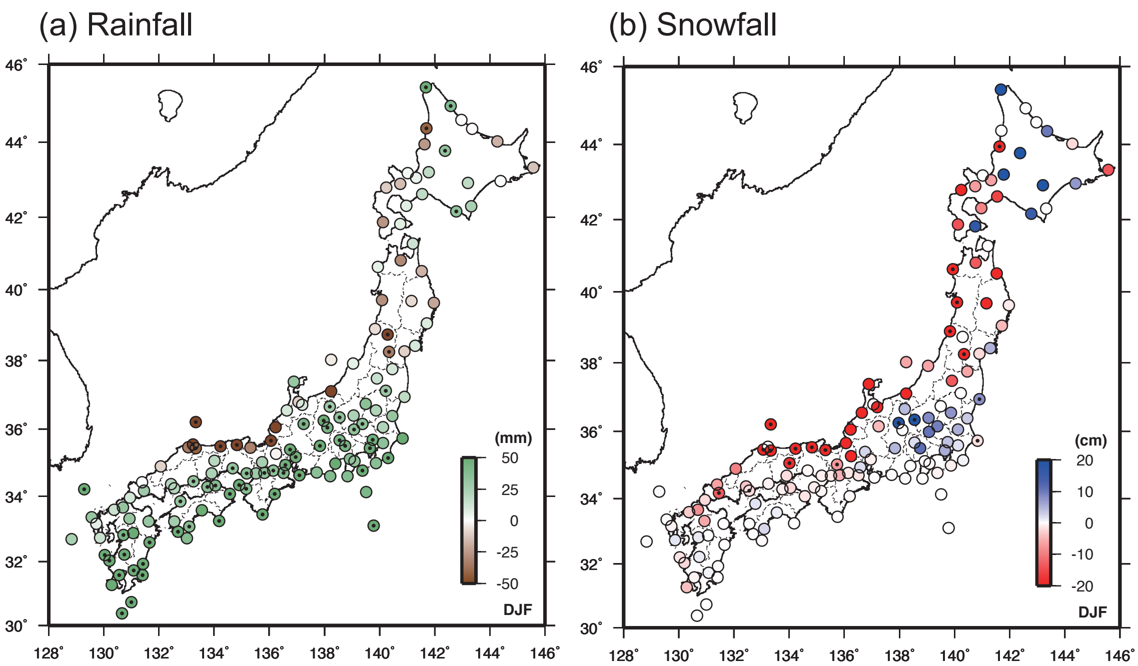

Fig. 4. Composited anomalies between the major El Niño and La Niña for total amounts of (a) rainfall and (b) snowfall in boreal winter. The values are three-month integration of daily-based data. Stations with a confidence level of > 95% are denoted by dot.

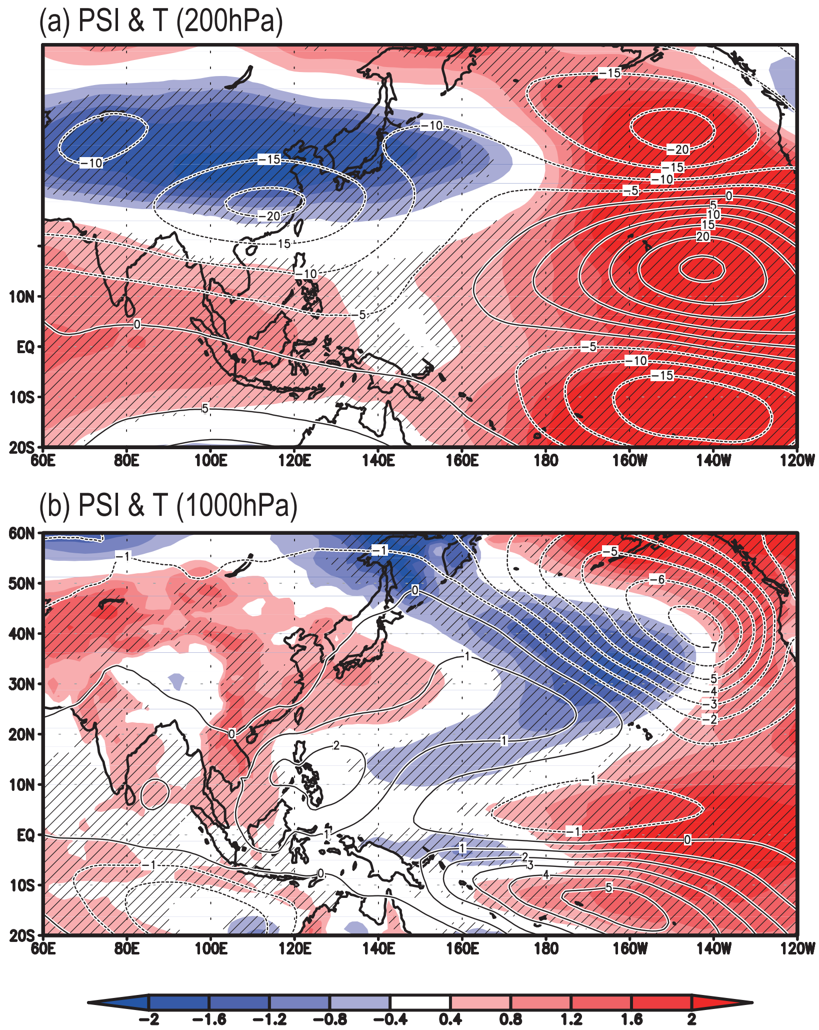

Fig. 5. Same as Fig. 4 but for stream function (contours: positive indicates anti-cyclone in the Northern Hemisphere) and temperature (shading); (a) 200 hPa, (b) 1000 hPa. Areas with a confidence level of > 95% are denoted by oblique line.

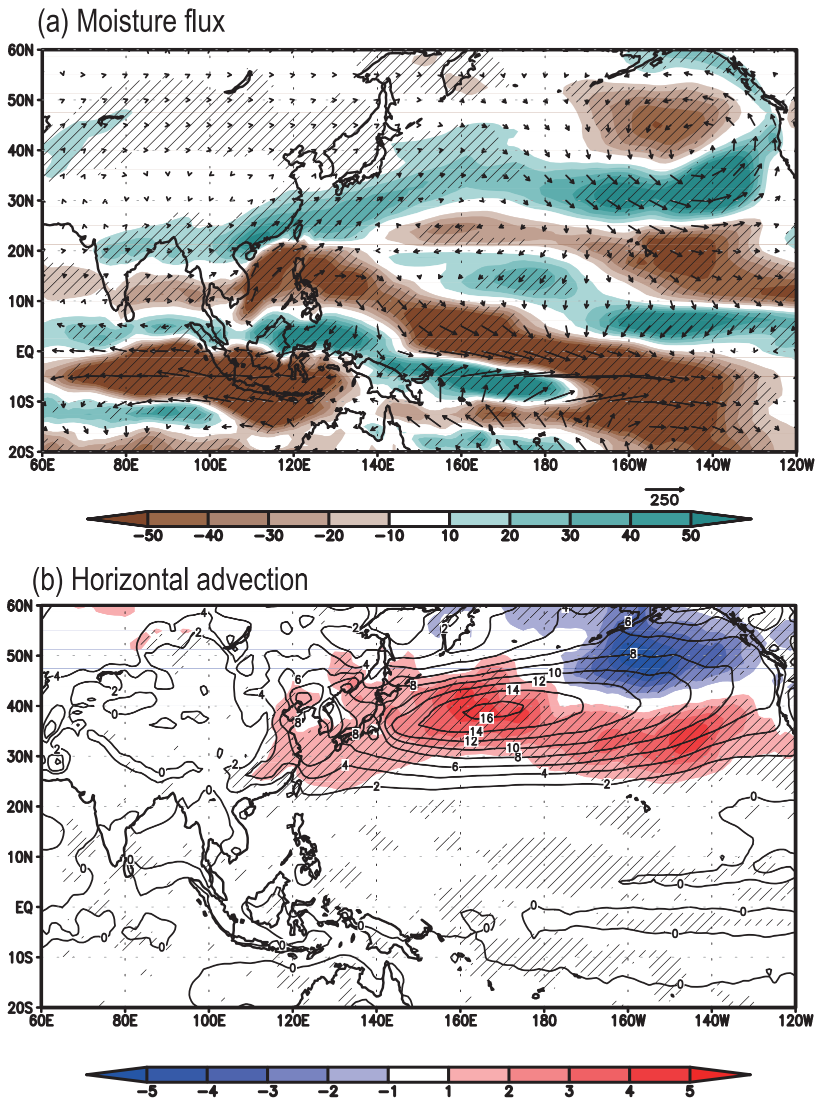

Fig. 6. Same as Fig. 4 but for (a) vertically integrated moisture flux (q'u', q'v') in the lower troposphere (1000-1hPa) and (b) horizontal heat advection (v'T') at 850 hPa. Areas with a confidence level of > 95% are denoted by oblique line.

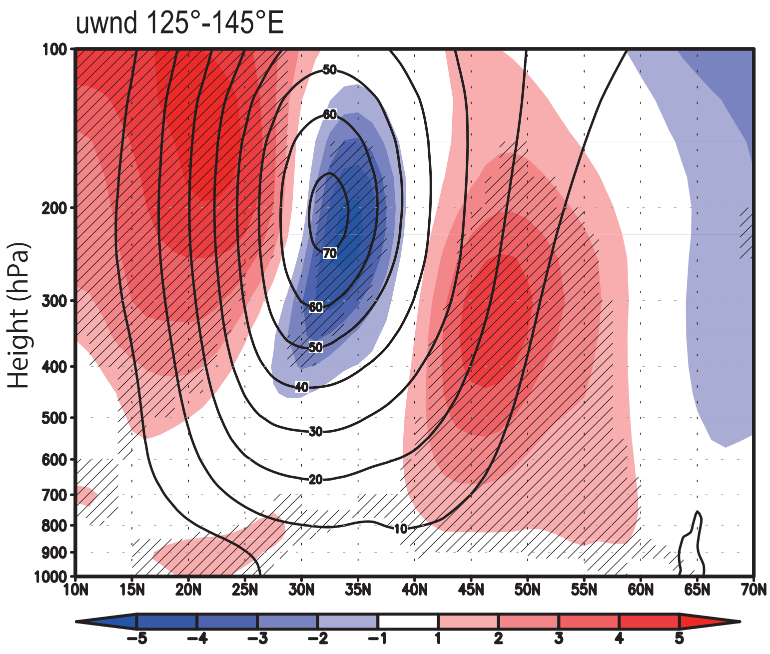

Fig. 7. Latitude-height section of the zonal mean u-wind (m s-1) across Japan (125°-145°E), showing the STJ. Shading denotes composited anomalies between the major El Niño and La Niña. Contours indicate the climatology. Areas with a confidence level of > 95% are denoted by oblique line.

Table 1. DJF composited anomalies between the top 10 El Niño minus La Niña events. Bold indicates a confidence level > 95%. Rainfall and snowfall anomalies were provided by the Tokyo Meteorological Observatory. Horizontal advection (*v'T'*) at 850 hPa and vertically (1000-1hPa) integrated moisture flux is the area average over 25°–35°N and 120°–140°E. The STJ is a zonal wind component at 200 hPa averaged over 30°–35°N and 120°–140°E.

	El Niña	La Niña	Difference
Pacific coast cyclones	**11.0**	**7.6**	3.4
rainfall (mm)	**198.7**	151.8	46.9
snowfall (cm)	8.2	**4.4**	3.8
moisture flux ($kgms\text{-}^{1}$)	**159.1**	140.7	18.4
v'T' (850hPa)	**6.2**	**5.2**	1.0
STJ ($m\ s^{-1}$)	**67.8**	**70.3**	-2.5